RSC Advances

PAPER

View Article Online
View Journal | View Issue

Cite this: *RSC Adv.*, 2024, **14**, 10499

Cyclodextrin-conjugated low-molecular-weight polyethyleneimine as a macromolecular contrast agent for tumor-targeted magnetic resonance imaging

Guangkuo Liu,[ac] Xinxin Li,[ac] Xiaojie Liu,[c] Wangting Lu,[bc] Yanan Xue*[a] and Min Liu *[bc]

Macromolecular contrast agents (CAs) usually possess excellent contrast ability and tumor-targeting ability in comparison with small-molecule CAs, especially for early tumor detection. Herein, cyclodextrin-conjugated low-molecular-weight polyethyleneimine was synthesized as a macromolecular backbone. Afterward, a linear polymer with adamantane terminal and Gd chelates was synthesized, followed by conjugating with the backbone *via* host–guest interaction. Finally, folic acid was conjugated onto the as-prepared CAs through bioorthogonal chemistry, which endowed the CAs with the capability to accumulate into the tumor region. Compared to Magnevist (r_1 = 4.25 mM^{-1} s^{-1}) used in clinic, the PC/Ad-PEG_{2000}-PLL(DTPA-Gd)-FA exhibited higher longitudinal relaxivity (r_1 = 11.62 mM^{-1} s^{-1}) with excellent biocompatibility. Furthermore, *in vivo* experiments demonstrated that PC/Ad-PEG_{2000}-PLL(DTPA-Gd)-FA could effectively accumulate in the tumor region and produce a brighter image than that of Magnevist. The H&E staining and metabolic data further illustrated that this CA possessed excellent biocompatibility *in vivo*. Finally, these results above suggest that this macromolecular CA could be a potential candidate as a MRI CA for tumor-targeted diagnosis.

Received 12th January 2024
Accepted 20th March 2024

DOI: 10.1039/d4ra00316k

rsc.li/rsc-advances

1. Introduction

Cancer is now widely recognized as a global issue. Unfortunately, it lacks a global solution, with both the number of deaths and new cases increasing annually. According to the World Health Organization (WHO) estimates, over the next two decades, global cancer cases may increase by 60%, making the prevention and control situation crucial. Faced with this cancer incidence and mortality, governments around the world are under immense pressure and challenges.[1–4]

Molecular imaging is a highly sensitive and specific imaging method that visualizes, characterizes, and detects biological processes at the molecular and cellular levels in humans or other living organisms in a non-invasive manner, which is widely used in the clinic.[5–7] Among them, Magnetic Resonance Imaging (MRI) visualizes images by detecting the distribution of hydrogen ions under a pulse magnetic field. The MRI technique possesses lots of advantages, including high spatial resolution for soft tissues, no ionizing radiation, the ability to simultaneously observe axial and sagittal planes, and the ability to reflect subtle differences in lesions between tissues. However, the MRI technique also possesses some disadvantages, including lower sensitivity and limited ability to detect small lesions. Therefore, we usually use CAs to enhance the contrast resolution in the clinic.[8–14]

Currently, the CAs used in clinical practice are mainly small molecule gadolinium complexes, such as Magnevist.[15] These small molecule gadolinium complexes are pioneers in enhancing MRI imaging quality. However, these small molecule CAs also have some significant drawbacks *in vivo*, including low relaxivity, short circulation time in the blood, brief residence time in tissues, and lack of targeting specificity, which fails to meet the demands for early tumor detection.[16,17] According to Bloembergen's relaxation theory, factors such as rotational correlation time, the number of coordinated water molecules, exchange rate of inner and outer shell water molecules, and the distance between coordinated water and the paramagnetic metal center are crucial in influencing relaxivity. Therefore, modifying small molecule CAs into macromolecular CAs is an important approach to enhance their imaging efficacy. This method helps improve relaxivity, prolong residence time in the body, and enhance targeting specificity for a particular tissue or lesion, thereby better meeting the requirements for early tumor diagnosis.[8,9,18]

[a]*Hubei Key Laboratory for Novel Reactor and Green Chemistry Technology, School of Chemical Engineering and Pharmacy, Wuhan Institute of Technology, Wuhan 430205, China*

[b]*State Key Laboratory of Precision Blasting, Jianghan University, Wuhan, 430056, China. E-mail: mliu2018@jhun.edu.cn*

[c]*School of Optoelectronic Materials & Technology, Institute for Interdisciplinary Research, Jianghan University, Wuhan, 430056, China*

Polyethylenimines (PEIs) are cationic polymers with a high content of amino groups, which endowed PEIs with wide use in different applications. PEIs with high molecular weight exhibited a severe cytotoxicity and reduced blood compatibility. Therefore, low molecular weight PEIs were usually used.[19–21] β-cyclodextrin, one of the cyclic oligosaccharides, contains lots of active hydroxy groups and can form stable inclusion complexes with molecular guests in aqueous solution.[22–25] Therefore, combination of low molecular weight PEIs with β-cyclodextrin has been demonstrated to be an improved way to obtain a multifunctional macromolecule. The as-prepared macromolecule not only decreases the toxicity of PEIs, but also offers lots of active sites which can interact with certain molecules, such as adamantane.[26–29]

Herein, cyclodextrin-conjugated low-molecular-weight polyethyleneimine was prepared as a backbone. Thereafter, a linear polymer with adamantane terminal and Gd chelates was conjugated onto the macromolecule backbone through host–guest interaction, followed by conjugation with folic acid through click chemistry. Our result illustrated that this as-prepared CA possessed excellent biocompatibility and could effectively accumulate in the tumor region and produced a bright image with excellent biocompatibility.

2. Materials and methods

2.1 Materials

1,1-Carbonyldiimidazole (CDI), branched polyethylenimine (PEI, $M_w = 800$ Da), and folic acid were purchased from Sigma-Aldrich. $GdCl_3 \cdot 6H_2O$ was purchased from Tokyo Chemical Industry. N_3-PEG_{2000}-NH_2 was obtained from Xiamen Sinopeg Biotech CO., Ltd. Cyclodextrin underwent recrystallization three times in water, and was stored in a vacuum drying oven at 60 °C before use. DBCO-PEG_{2000}-NH_2 was purchased from Xi'an Confluore Biological Technology Co., Ltd. Ad-PEG_{2000}-PLL(DTPA-Gd)-N_3 and DBCO-PEG_{2000}-FA were synthesized in our lab.[30] All the other reagents were obtained from the domestic suppliers.

^{1}H NMR spectra were obtained using a Varian NMR spectrometer at 400 MHz. Gel permeation chromatography (GPC) measurements were carried out using an Agilent PL-GPC50/Agilent 1260, 0.15 M $NaNO_3$ water solution was used as an eluent with a flow rate of 1 mL min^{-1}. The Gd concentrations of the samples were detected *via* an inductively coupled plasma optical emission spectrometer (ICP-OES, Agilent 720ES). The *in vitro* T_1-weighted data were obtained *via* a 0.5*T* NMR-analyzer, while the *in vivo* T_1-weighted MR images were acquired on a 4.7*T* scanner (Bruker).

2.2 Synthesis of PEI_{800}-CyD

The PEI_{800}-CyD (PC) backbone was synthesized according to the previous method with minor revision.[31–34] Briefly, recrystallized β-CD (2.1 g, 1.85 mmol) and CDI (2.4 g, 14.8 mmol) were dissolved in anhydrous DMF (10 mL), and the mixture was stirred at room temperature for 1 h under N_2 atmosphere. Afterward, the mixture was precipitated into cold ether (150 mL), the precipitate was collected through filtration and washed three times with ether. Next, the activated CyD was dissolved in anhydrous DMSO (10 mL), which was then added dropwise into a DMSO (10 mL) solution containing PEI_{800} (2.9 g, 3.63 mmol) and triethylamine (4.14 mL, 29.6 mmol). After stirring overnight, the resulting mixture was dialyzed (RC Dialysis Membrane, MWCO: 8–14 kD) against water for 3 days. Finally, the dialysis solution was filtered to remove insoluble cross-linked polymer, followed by lyophilization to obtain the final product (PEI-CyD, 1.77 g, stored at −20 °C). The molecular weight (M_w) of PC polymer was determined to be 3.4×10^4 g mol^{-1} with the PDI index of 2.8.

2.3 Synthesis of PC/Ad-PEG_{2000}-PLL(DTPA-Gd)-FA

PC (5 mg) was dissolved in ultrapure water (10 mL). Ad-PEG_{2000}-PLL(DTPA-Gd)-N_3 (64 mg) was dissolved in another ultrapure water (10 mL), and then this solution was added dropwise into the above solution and stirred overnight. Next, the resulting mixture (PC/Ad-PEG_{2000}-PLL(DTPA-Gd)-N_3) was purified through an ultrafiltration process (Millipore, $M_w = 50\,000$, 5000 rpm) to remove the unreacted Ad-PEG_{2000}-PLL(DTPA-Gd)-N_3.

Next, DBCO-PEG_{2000}-FA (5 mg) was dissolved into 100 μL deionized water, followed by adding to the above solution, and then stirred overnight to facilitate the click reaction between DBCO-PEG_{2000}-FA and PC/Ad-PEG_{2000}-PLL(DTPA-Gd)-N_3. The obtained solution (PC/Ad-PEG_{2000}-PLL(DTPA-Gd)-FA) was then purified through an ultrafiltration (Millipore, $M_w = 10\,000$, 5000 rpm) process to remove the unreacted DBCO-PEG_{2000}-FA. Finally, the Gd concentration of the final solution was detected *via* ICP-OES.

2.4 Relaxivity measurement

PC/Ad-PEG_{2000}-PLL(DTPA-Gd)-FA solutions with different concentrations of gadolinium ions (0.25, 0.5, 1, 1.5, 2 mM) was prepared, the T_1 relaxivity and T_1-weighted images were acquired with spinecho acquisition, and Magnevist was used as control. The parameters were set as follows: T_R (repetition time) = 100.0 ms, T_E (echo time) = 8.6 ms, NS (number of scans) = 1.

2.5 Cell viability assessment using CCK-8 assay

In order to evaluate the cytotoxicity of PC/Ad-PEG_{2000}-PLL(DTPA-Gd)-FA, a comprehensive analysis was conducted using the Cell Counting Kit-8 (CCK-8) assay. Mouse breast cancer cells (4*T*1) were cultured in RPMI 1640 medium containing 10% fetal bovine serum (FBS), 1% penicillin and streptomycin at 37 °C and 5% CO_2 in a cell culture incubator.

Briefly, 4*T*1 cells were introduced into a 96-well plate at a seeding density of 8000 cells in 100 μL of medium per well and incubated till their confluency reached about 80%. Next, in order to evaluate the cytotoxic effects of PC/Ad-PEG_{2000}-PLL(DTPA-Gd)-FA, various concentrations of Gd ions (6, 3, 1.5, 0.75 mM) were prepared by diluting the solution of PC/Ad-PEG_{2000}-PLL(DTPA-Gd)-FA. These varying concentrations of the contrast agent were then introduced to their respective wells, with each well receiving 100 μL of the prepared solution. The control group was added with 100 μL of medium. The cells were then subjected to

an additional incubation period of 24 hours. Following the incubation, the medium in each well was replaced with 100 μL of fresh medium. Subsequently, 10 μL of the CCK-8 reagent was added to each well, and the plate was returned to the cell culture incubator for a 2 hours incubation period. The absorbance at 450 nm was measured with microplate reader.

2.6 Hematoxylin–eosin (H&E) staining analysis

Hematoxylin and eosin (H&E) staining was carried out to further evaluated the toxic of PC/Ad-PEG$_{2000}$-PLL(DTPA-Gd)-FA *in vivo*. All animal procedures were performed in accordance with the Guidelines for Care and Use of Laboratory Animals of Jianghan University and approved by the Animal Ethics Committee of Jianghan University. A total of nine four-week-old female nude mice were acclimatized for 1 week under SPF conditions, provided with a standard diet and purified water. The nude mice were divided into three groups ($n = 3$), and two of the groups were intraperitoneally injected with 100 μL of physiological saline containing PC/Ad-PEG$_{2000}$-PLL(DTPA-Gd)-FA at gadolinium ion concentrations of 0.1 mmol kg^{-1} and 0.3 mmol kg^{-1}, respectively. The third group was injected with 100 μL of physiological saline as a control. After being continuously fed for 2 days, the mice were euthanized using cervical dislocation, and their organs, including the heart, liver, spleen, lungs, and kidneys, were collected and soaked in formalin. Finally, histological staining was carried out to analyze these organs.

2.7 *In vivo* MR imaging

4*T*1 cells were digested with trypsin and collected by centrifugation (1000 rpm, 5 min) followed by washing with PBS. Next, 100 μL of the prepared 4*T*1 cell (1×10^6/100 μL) suspension was injected subcutaneously into the empty cavity of the right hind limb of the nude mouse using a syringe. The inoculated nude mice were kept under SPF conditions and the growth of the tumors was observed until they reached 8 mm in diameter after 10 days of cell implantation.

Nine four-week-old female nude mice were acclimatized to SPF conditions for a week before the experiments commenced. For *in vivo* imaging: the nine tumor-bearing nude mice were divided into three groups ($n = 3$), and 135 μL of 25% urethane solution was injected into the peritoneal cavity to anesthetize the tumor-bearing nude mice. Next, the mice were fixed on a fixture and placed in a 4.7*T* Magnetic Resonance Imaging (MRI) machine. Prior to the imaging procedure, blank scans were conducted, and the resultant images served as reference blanks. The temperature within the imaging setup was consistently maintained at 35 °C. Subsequently, PC/Ad-PEG$_{2000}$-PLL(DTPA-Gd)-FA, PC/Ad-PEG$_{2000}$-PLL(DTPA-Gd), and Magnevist in physiological saline solutions were injected through the tail vein, with a gadolinium ion concentration of 0.1 mmol kg^{-1} for each group. After injection, the nude mice were transferred to the 4.7*T* MRI machine to observe the MRI imaging of the tumor. To assess the MRI imaging results, the relative brightness of each group was compared with the corresponding blank reference. The blank reference's brightness was standardized to a value of 1. This comparison was carried out for each group at the same time point, allowing for a quantitative evaluation of the imaging outcomes.

2.8 Biodistribution assay *in vivo*

Three four-week-old female nude mice were selected for this biodistribution assay. 100 μL of a physiologic saline solution of PC/Ad-PEG$_{2000}$-PLL(DTPA-Gd)-FA, with a concentration of 0.1 mmol kg^{-1} of gadolinium ion was injected *via* tail vein. After continuing to feed the mice in a SPF environment for 10 days, these mice were euthanized using cervical dislocation, and their heart, lungs, liver, spleen and kidney were collected and weighed. Then, the organs and tissues were completely digested in 5 mL Lefort aqua regia by heating. The supernatant was fixed to 10 mL and the Gd content in each organ or tissue was determined by ICP-MS. The retention of gadolinium in various organs/tissues was presented as the percentage of the injected dose per organ of tissue (% ID).

2.9 Statistical analysis

The obtained results were subjected to statistical analysis utilizing the OriginPro 8.5 software, and the results are presented as mean ± standard deviation (SD). A significance level of $p < 0.05$ was considered statistically significant.

3. Results and discussion

3.1 Synthesis and characterization of PC/Ad-PEG$_{2000}$-PLL(DTPA-Gd)-FA

In this study, cyclodextrin-conjugated low-molecular-weight polyethyleneimine was used to construct a tumor-targeted macromolecular MRI CA *via* host–guest interaction (as shown in Scheme 1). First of all, the hydroxyl of β-cyclodextrin was activated by 1,10-carbonyldiimidazole (CDI), followed by the reaction with the primary amine of low-molecular-weight PEI to form PEI-CyD, which possessed numerous active sites for the anchoring of adamantine derivative. Next, N_3-PEG-NH_2 was used to initiate the ring-opening polymerization of lysine-NCA, followed by conjugation of adamantine and Gd chelates. Finally, the as-prepared CA was assembled through host–guest interaction between β-cyclodextrin and adamantine, and then targeting ligand was conjugated *via* click chemistry.

The ^{1}H NMR spectrum of PEI-CyD was shown in Fig. 1, the characteristics peak (δ 2.8–2.2) belonged to PEI ethylene protons (–$CH_2CH_2NH_2$–), while the C1 proton and C2–C6 protons of CyD appeared at δ 5.0 and δ 3.0–4.2, respectively. By comparing the peak area ratio of CyD to PEI, 32% of hydroxyl groups in the ring of CyD were activated by CDI, which means that 2–3 hydroxyl groups per each CyD were reacted with PEI.

3.2 Longitudinal relaxivity and MR images *in vitro*

To investigate the potential of PC/Ad-PEG$_{2000}$-PLL(DTPA-Gd)-FA as an MRI CA, longitudinal relaxivity was measured *via* a 0.5*T* MRI scanner at 35 °C. The r_1 value was calculated from the slope of curves. As shown in Fig. 2a, the r_1 relaxivity of Magnevist is 4.25 mM^{-1} s^{-1}, while it is 11.62 mM^{-1} s^{-1} for PC/Ad-PEG$_{2000}$-

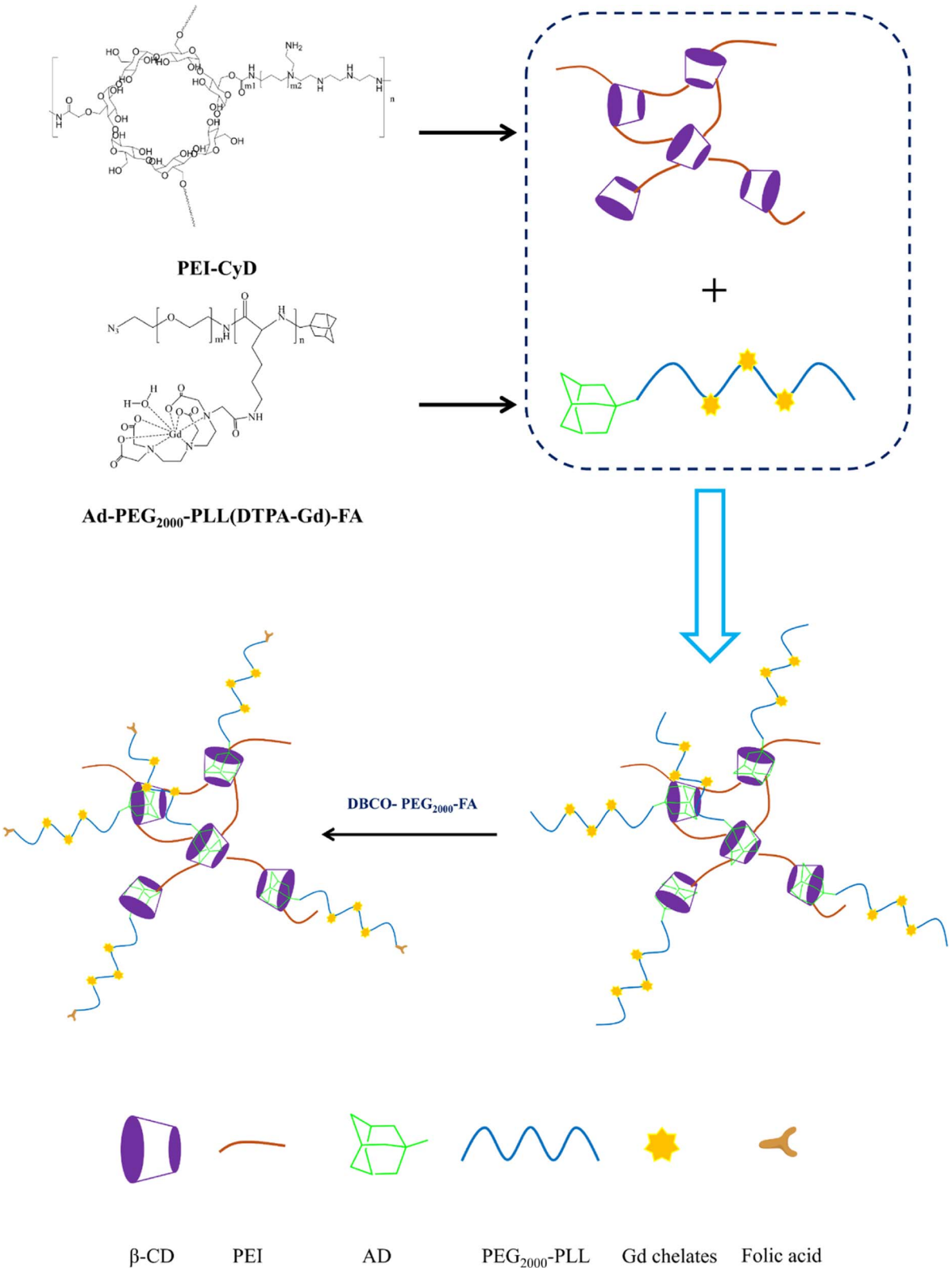

Scheme 1 The synthesis procedure of PC/Ad-PEG_{2000}-PLL(DTPA-Gd)-FA.

PLL(DTPA-Gd)-FA, up to 2.7 times higher than that of Magnevist.

In addition, T_1-weighted MR images of PC/Ad-PEG_{2000}-PLL(DTPA-Gd)-FA with various Gd^{3+} concentration were carried out to further confirm the results above, Magnevist and water

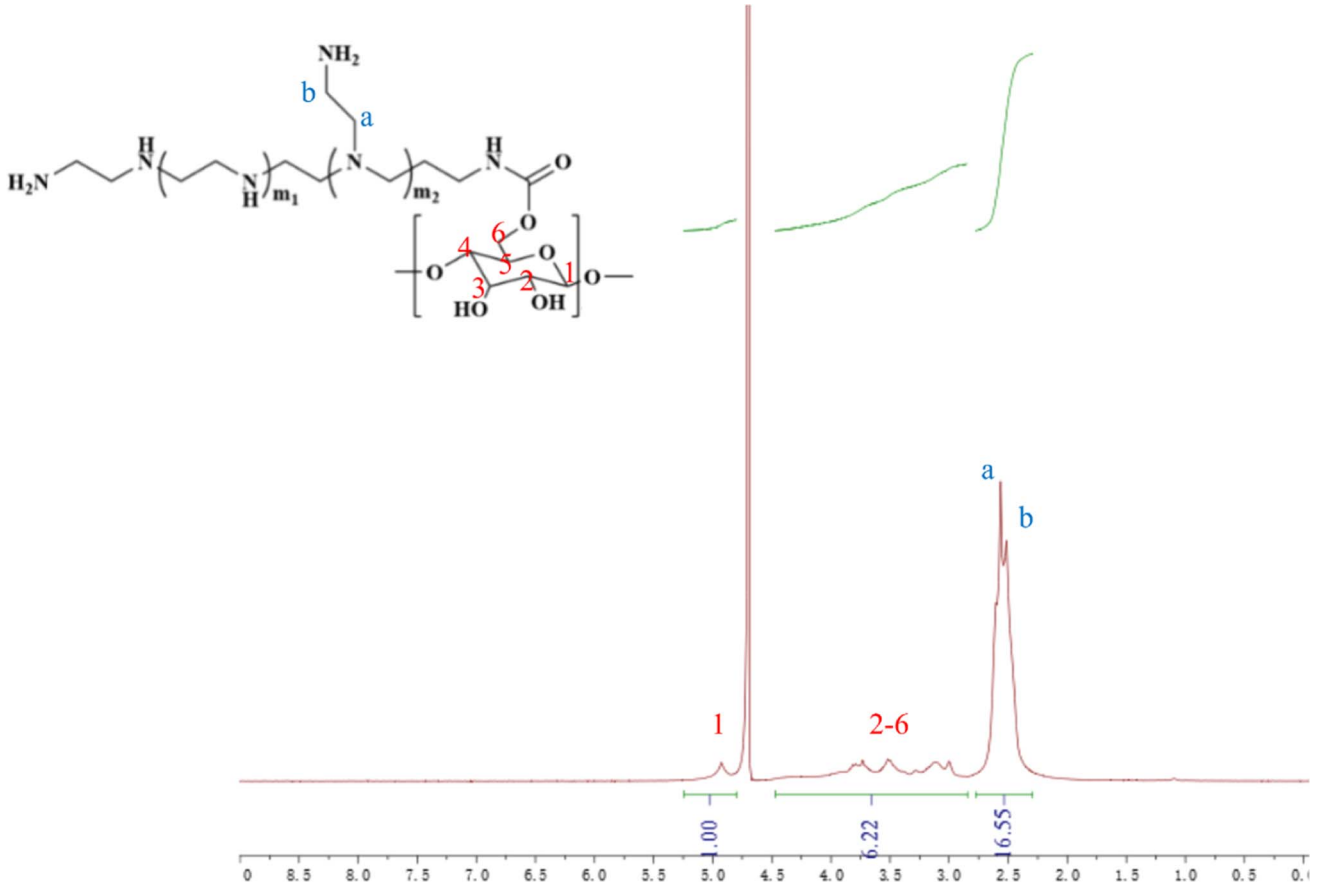

Fig. 1 ^{1}H NMR spectrum of PEI-CyD.

were chosen as the controls. As shown in Fig. 2b, the brightness of the light spot is positively correlated with its concentration, with the increase of concentration of Gd^{3+}, the brightness was obviously increased. Moreover, the brightness of sample was much higher than that of Magnevist at each Gd^{3+} concentration.

According to the Bloembergen-Solomon-Morgan theory, relaxivities of the CAs are closely related to the rotational correlation time (τ_R) of complexes. Therefore, increasing the molecular size can slow down the rotational motion of the complex, thus enhancing the rotational correlation time (τ_R), and thereby increasing the relaxivity.[8,9] In this work, Gd-chelates were conjugated onto the PLL segment followed by conjugating onto PC backbone through host–guest interaction. This modification method not only enhance the rotational correlation time (τ_R), but also improve the loading density of Gd chelates.

3.3 Toxicity assay

As a medication used for treating living organisms, the importance of its biological safety is self-evident. First of all, CCK-8 assay was used to investigate the cytotoxicity of PC/AD-PEG_{2000}-PLL(DTPA-Gd)-FA to 4*T*1 cells. The result was shown in Fig. 3, the cytotoxicity of PC/AD-PEG_{2000}-PLL(DTPA-Gd)-FA against 4*T*1 cells was found to be over 100% below 3 mM, and the viability remained over 90% even when the Gd^{3+} concentration went up to 6 mM. This result suggest that the as-prepared CA has good biocompatibility.

Next, H&E staining was carried out to verify whether PC/AD-PEG_{2000}-PLL(DTPA-Gd)-FA has any *in vivo* tissue toxicity. Microscopic images of tissue sections after H&E staining are shown in Fig. 4. The experimental results indicated that there was no significant damage to the mouse tissue organs after the injection of 0.1 mM kg^{-1} and 0.3 mM kg^{-1} of PC/AD-PEG_{2000}-PLL(DTPA-Gd)-FA. No necrosis was evident in cardiac cells, and there were no indications of inflammation in hepatic cells, fibrosis in pulmonary cells, or morphological changes in renal cells. The examined organs, such as the heart, liver, spleen, lungs, and kidneys, displayed minimal histological alterations and maintained a normal histological morphology. Combined the results above, it can be concluded that PC/AD-PEG_{2000}-PLL(DTPA-Gd)-FA possesses excellent biocompatibility.

3.4 *In vivo* MR imaging

In the above section, we have already characterized the basic properties of PC/AD-PEG_{2000}-PLL(DTPA-Gd)-FA *in vitro*. However, *in vivo* MR imaging efficacy against FR-positive tumors is a critical criterion for evaluating CAs. Thereafter, mice bearing 4*T*1 xenografts were randomly divided into three groups, Magnevist, PC/AD-PEG_{2000}-PLL(DTPA-Gd), PC/AD-PEG_{2000}-PLL(DTPA-Gd)-FA.

First of all, transverse T_1-weighted MR images of the tumor-bearing mice were acquired before injection which was set as blank. Afterward, the mice were tail-vein injected with samples,

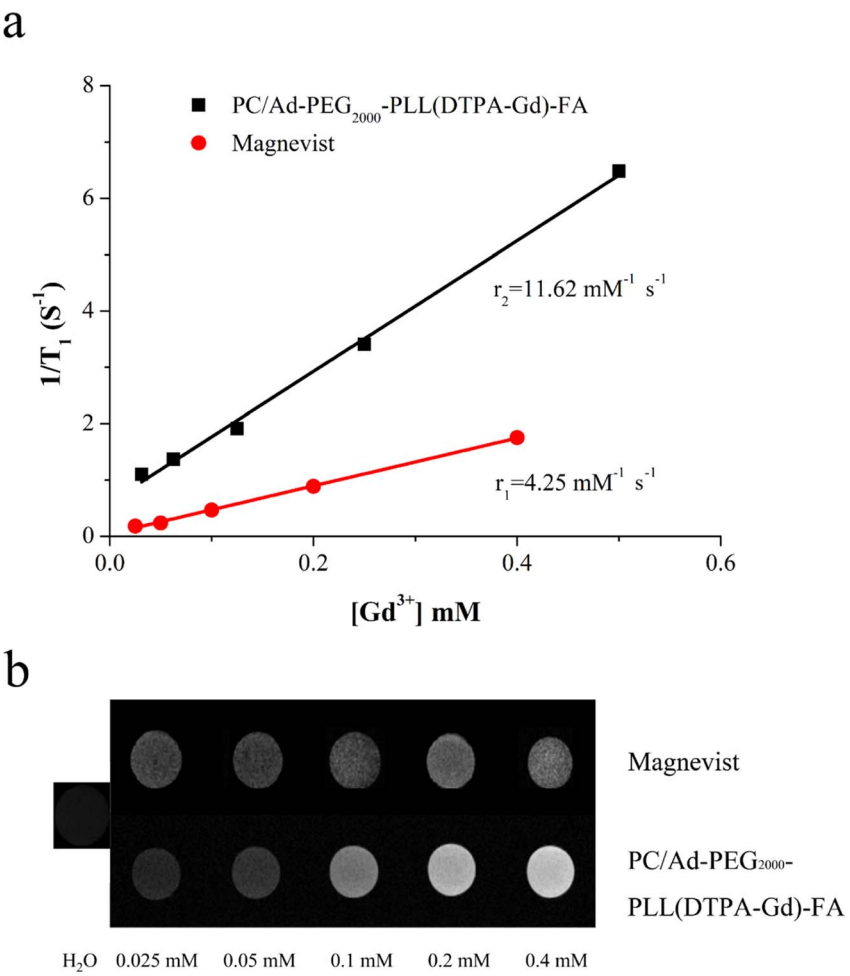

Fig. 2 (a) Longitudinal relaxation rate ($1/T_1$) of PC/Ad-PEG_{2000}-PLL(DTPA-Gd)-FA, and Magnevist. (b) T_1-weighted MR images of PC/Ad-PEG_{2000}-PLL(DTPA-Gd)-FA, and Magnevist at different Gd^{3+} concentrations. H_2O was used as control.

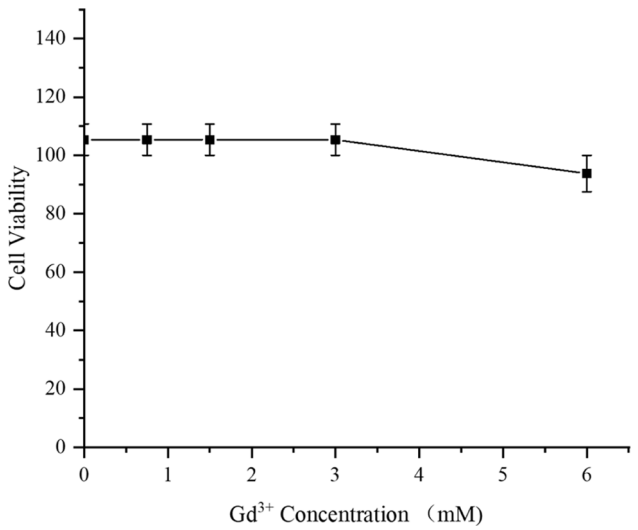

Fig. 3 CCK-8 assay of PC/AD-PEG_{2000}-PLL(DTPA-Gd)-FA in 4T1 cells.

and then the transverse T_1-weighted MR images were acquired 2 h after injection. As illustrated in Fig. 5, for the Magnevist group and PC/AD-PEG_{2000}-PLL(DTPA-Gd) group, there is no significant difference in the images between the blank and 2 h after injection. However, a noticeable contrast emerged for the PC/AD-PEG_{2000}-PLL(DTPA-Gd)-FA group. The brightness produced by the samples follows the order: PC/AD-PEG_{2000}-PLL(DTPA-Gd)-FA > PC/AD-PEG_{2000}-PLL(DTPA-Gd) > Magnevist.

To facilitate a more convenient and accurate assessment, quantitative signal analysis was conducted using ImageJ software. As shown in Fig. 6, there is minimal brightness change at the tumor site for the Magnevist, PC/AD-PEG_{2000}-PLL(DTPA-Gd) groups, with values up to 1.07–1.13 times higher than those of precontrast images. However, the tumor treated with PC/AD-PEG_{2000}-PLL(DTPA-Gd)-FA exhibited a 1.3-fold increase compared to the precontrast image. These findings suggest that folic acid can contribute to the cell uptake of nanoparticle in the FR-positive tumors, promoting their accumulation in the tumor region and consequently enhancing the contrast brightness in that area and maintain for a period of time.

The CCK-8 and H&E assay have already demonstrated the excellent biocompatibility of the as-prepared CA. *In vivo* imaging results further support its ability to produce bright signals in the tumor region. However, the metabolism of the CA *in vivo* is a crucial aspect to consider. CA has the potential to accumulate

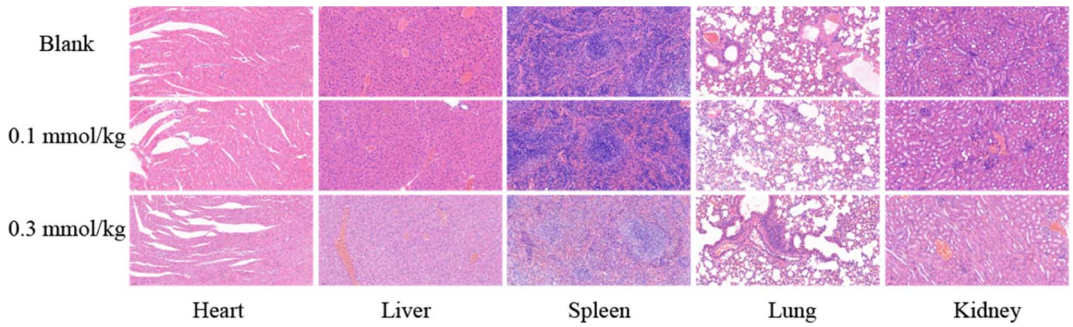

Fig. 4 H&E-stained tissue sections from mice injected with PC/AD-PEG_{2000}-PLL(DTPA-Gd)-FA at different dose of Gd^{3+} (0.1 mmol kg^{-1}, 0.3 mmol kg^{-1}) 2d postinjection and mice injected with physiological saline were used as control.

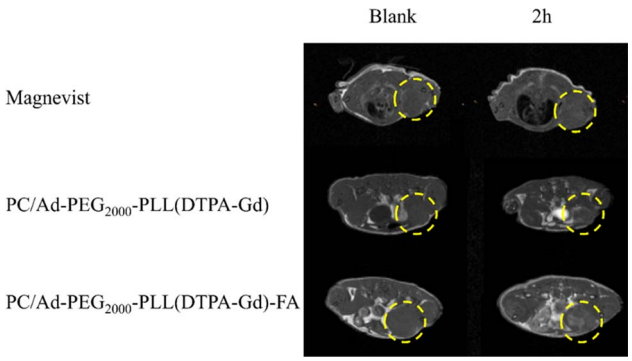

Fig. 5 Transverse MR images of tumor-bearing mice injected with Magnevist, PC/AD-PEG_{2000}-PLL(DTPA-Gd), PC/AD-PEG_{2000}-PLL(DTPA-Gd)-FA at Gd dose of 0.1 mmol kg^{-1}. The yellow dot circle shows the location of tumor.

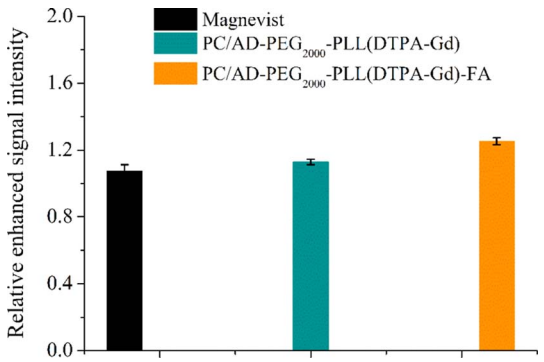

Fig. 6 Quantitative analysis of MR signal intensity of Magnevist, PC/AD-PEG_{2000}-PLL(DTPA-Gd), PC/AD-PEG_{2000}-PLL(DTPA-Gd)-FA before injection and 2 h post injection through ImageJ software.

in the body, posing a risk of inducing nephrogenic systemic fibrosis in patients with renal insufficiency. Therefore, we assessed the residual amounts of the synthesized macromolecular CA (PC/AD-PEG_{2000}-PLL(DTPA-Gd)-FA) in major organs. Five-week-old nude mice were used, and after injection of the CA at a dose of 0.1 mmol kg^{-1} for 7 days, we collected the heart, liver, spleen, lung, kidney for Gd residue measurement. As shown in Fig. 7, The residual amounts of Gd in the heart, liver, spleen, lung, and kidney were 0.01%, 0.28%, 0.03%, 0.02%, and 0.02%

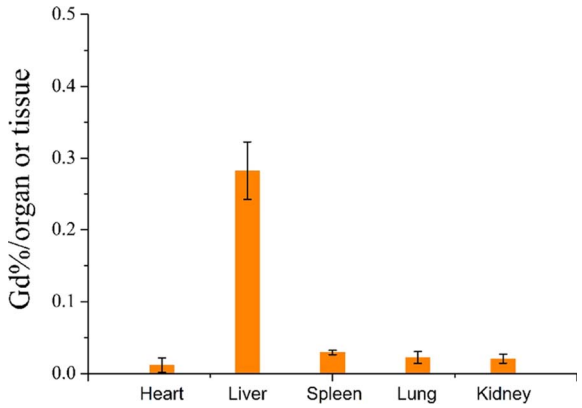

Fig. 7 Retention of Gd^{3+} in the tumor and main organs of mice 7 days after intravenous injection of PC/AD-PEG_{2000}-PLL(DTPA-Gd)-FA at the dose of 0.1 mmol Gd per kg.

per tissue or organ, respectively. These data indicate that the prepared macromolecular CA exhibits minimal long-term residue in major organs and tissues, meeting the initially requirements for long-term safety of CA *in vivo*.

4. Conclusions

In this work, a macromolecular CA (PC/AD-PEG_{2000}-PLL(DTPA-Gd)-FA) was synthesized and well characterized both *in vitro* and *in vivo*, which possessed a higher longitudinal relaxivity (r_1 = 11.62 mM^{-1} s^{-1}), up to 2.7 times higher than that of Magnevist. Toxicity assay and biodistribution assay *in vivo* illustrated that PC/AD-PEG_{2000}-PLL(DTPA-Gd)-FA possessed excellent biocompatibility. *In vivo* MR imaging further demonstrated that the PC/AD-PEG_{2000}-PLL(DTPA-Gd)-FA can enhance the contrast brightness in the tumor area and maintain for a period of time in comparison with the non-targeted CA and commercial Magnevist. Therefore, PC/AD-PEG_{2000}-PLL(DTPA-Gd)-FA will be a potential CA with excellent biocompatibility for tumor diagnosis.

Author contributions

Guangkuo Liu and Xinxin Li contribute equally to this manuscript. The manuscript was written through contributions from all authors.

Conflicts of interest

The author declare that they have no known competing financial interest.

Acknowledgements

This project was funded by the Excellent Discipline Cultivation Project of Jianghan University (2023XKZ039). Project of State Key Laboratory of Precision Blasting (PBSKL2022202).

References

1 Z. Lu, Y. Chen, D. Liu, X. Jiao, C. Liu, Y. Wang, Z. Zhang, K. Jia, J. Gong, Z. Yang and L. Shen, *Nat. Med.*, 2023, **29**, 3022–3032.
2 H. Sung, J. Ferlay, R. L. Siegel, M. Laversanne, I. Soerjomataram, A. Jemal and F. Bray, *Ca-Cancer J. Clin.*, 2021, **71**, 209–249.
3 J. Shi, P. W. Kantoff, R. Wooster and O. C. Farokhzad, *Nat. Rev. Cancer*, 2017, **17**, 20–37.
4 P. Jiang, S. Sinha, K. Aldape, S. Hannenhalli, C. Sahinalp and E. Ruppin, *Nat. Rev. Cancer*, 2022, **22**, 625–639.
5 W. J. G. Oyen and W. T. A. van der Graaf, *Nat. Rev. Clin. Oncol.*, 2009, **6**, 609–611.
6 A. V. Naumova, M. Modo, A. Moore, C. E. Murry and J. A. Frank, *Nat. Biotechnol.*, 2014, **32**, 804–818.
7 T. F. Massoud and S. S. Gambhir, *Genes Dev.*, 2003, **17**, 545–580.
8 P. Caravan, *Chem. Soc. Rev.*, 2006, **35**, 512–523.
9 P. Caravan, J. J. Ellison, T. J. McMurry and R. B. Lauffer, *Chem. Rev.*, 1999, **99**, 2293–2352.
10 L. M. De Leon-Rodriguez, A. J. M. Lubag, C. R. Malloy, G. V. Martinez, R. J. Gillies and A. D. Sherry, *Acc. Chem. Res.*, 2009, **42**, 948–957.
11 J. Gallo, N. J. Long and E. O. Aboagye, *Chem. Soc. Rev.*, 2013, **42**, 7816–7833.
12 B. Chen, L. Liu, R. Yue, Z. Dong, C. Lu, C. Zhang, G. Guan, H. Liu, Q. Zhang and G. Song, *Nano Today*, 2023, **51**, 101931.
13 A. Banerjee, B. Blasiak, A. Dash, B. Tomanek, F. C. J. M. van Veggel and S. Trudel, *Chem. Phys. Rev.*, 2022, **3**, 011304.
14 S. Fu, Z. Cai and H. Ai, *Adv. Healthc. Mater.*, 2021, **10**, 2001091.
15 H. Niendorf, *Bristol Medico-Chirurgical J.*, 1988, **103**, 34.
16 J. Tang, Y. Sheng, H. Hu and Y. Shen, *Prog. Polym. Sci.*, 2013, **38**, 462–502.
17 A. J. L. Villaraza, A. Bumb and M. W. Brechbiel, *Chem. Rev.*, 2010, **110**, 2921–2959.
18 T. J. Clough, L. Jiang, K.-L. Wong and N. J. Long, *Nat. Commun.*, 2019, **10**, 1420.
19 Q. Hu, F. Guo, F. Zhao, G. Tang and Z. Fu, *J. Biomater. Sci., Polym. Ed.*, 2017, **28**, 768–780.
20 C. Zhao and B. Zhou, *J. Funct. Biomater.*, 2023, **14**, 12.
21 S. Patnaik and K. C. Gupta, *Expert Opin. Drug Delivery*, 2013, **10**, 215–228.
22 G. R. Newkome, H. J. Kim, K. H. Choi and C. N. Moorefield, *Macromolecules*, 2004, **37**, 6268–6274.
23 A. Harada, *Acc. Chem. Res.*, 2001, **34**, 456–464.
24 X. Ma and Y. Zhao, *Chem. Rev.*, 2015, **115**, 7794–7839.
25 W.-L. Zhou, W. Lin, Y. Chen and Y. Liu, *Chem. Sci.*, 2022, **13**, 7976–7989.
26 B. Tian, Y. Liu and J. Liu, *Carbohydr. Polym.*, 2021, **251**, 116871.
27 Y. Shepelytskyi, C. J. Newman, V. Grynko, L. E. Seveney, B. Deboef, F. T. Hane and M. S. Albert, *Molecules*, 2020, **25**, 5576.
28 J. Wankar, N. G. Kotla, S. Gera, S. Rasala, A. Pandit and Y. A. Rochev, *Adv. Funct. Mater.*, 2020, **30**, 1909049.
29 Y.-M. Zhang, Y.-H. Liu and Y. Liu, *Adv. Mater.*, 2020, **32**, 1806158.
30 Y. Zhang, X. Li, X. Chen, Y. Zhang, Y. Deng, Y. Yu, B. Wang, Y. Xue, Y. Huang and M. Liu, *Mater. Des.*, 2022, **217**, 110620.
31 G. P. Tang, H. Y. Guo, F. Alexis, X. Wang, S. Zeng, T. M. Lim, J. Ding, Y. Y. Yang and S. Wang, *J. Gene Med.*, 2006, **8**, 736–744.
32 J. Shen, Q. Wang, Q. Hu, Y. Li, G. Tang and P. K. Chu, *Biomaterials*, 2014, **35**, 8621–8634.
33 S. Jain, S. Kumar, A. K. Agrawal, K. Thanki and U. C. Banerjee, *RSC Adv.*, 2015, **5**, 41144–41154.
34 Q. L. Hu, W. Li, X. R. Hu, Q. D. Hu, J. Shen, X. Jin, J. Zhou, G. P. Tang and P. K. Chu, *Biomaterials*, 2012, **33**, 6580–6591.